vation in cases where number of flops is an issue and for reasons just described.

The flop count for Jankovic's method when computing the first derivatives of p right eigenvectors with respect to q design parameters is given next for $[B] = [I]$.

1) Compute the first p left and right eigenvectors (same count as for EISPACK subroutines). : $3.5pN^2$
2) Compute $\{x_j\}\{x_j\}^T$ for $j = 1, \ldots, p$. : pN^2
3) LU decompose $[Q]^{-1} \equiv ([A] - \lambda_j[I] + \{x_j\}\{x_j\}^T)$. for $j = 1, \ldots, p$. : $pN^3/3$
4) For $j = 1, \ldots, p$ and $k = 1, \ldots, q$:
   a) Compute $[A]_{,k}\{x_j\}$ where κ is a sparsity parameter which is unity for full $[A]_{,k}$. : $pqN^2\kappa$
   b) Compute $[Q]([A]_{,k}\{x_j\})$. : pqN^2

The total number of flops is thus $[4.5p + pN/3 + pq(\kappa + 1)]N^2$. The flop count for computing the eigenvalues is not considered since the same count will appear in both methods to be compared. The flop count for the nth-order modal method is, on the other hand,

$$[3.5\hat{N} + N/3 + pq(\kappa + 1 + n)]N^2$$

The flop count for the nth-order modal method is thus smaller than that for Jankovic's method when

$$nq/N < z - 1/3p; \qquad z \equiv 1/3 + (4.5 - 3.5e)/N, \qquad e \equiv \hat{N}/p$$

As explained in the paper[2] (p. 386), a good value for e may be 3.0 for $N = 100$ which gives $z = 0.27$ and z increases for larger system sizes which makes the nth-order method more advantageous. For the first-order method, i.e., for $n = 1$, Jankovic's method is advantageous when only a single derivative is of interest, i.e., for $p = 1$. For larger number of eigenvector derivatives, the first-order method is preferable when the number of design parameters to be varied is not unusually high. On the other hand, the method $n = -1$ with the full set of eigenvectors used outperforms Jankovic's method when p is greater than about 10 or 11.

References

[1]Jankovic, M. S., "Comment on New Family of Modal Methods for Calculating Eigenvector Derivatives," *AIAA Journal*, Vol. 33, No. 5, 1995, pp. 965–967.

[2]Akgün, M. A., "New Family of Modal Methods for Calculating Eigenvector Derivatives," *AIAA Journal*, Vol. 32, No. 2, 1994, pp. 379–386.

Comment on "Induced Drag of Wings of Finite Aspect Ratio"

A. W. Bloy* and M. Jouma'a†
University of Manchester, Manchester M13 9PL, England, United Kingdom

In Ref. 1 Lam modifies lifting-line theory using an approximate model of wing wake roll up to determine the effect of roll up on induced drag. Elliptic wing loading is considered, and the wake model consists of a flat trailing vortex sheet of finite length. This vortex sheet is assumed to roll up suddenly at some distance ℓ downstream to form two discrete trailing vortices which, for elliptic loading, are spaced a distance of $\pi/4$ times the wing span apart. However this roll-up model allows the vortex lines which trail in the freestream direction to end in the fluid at the downstream position at which the sudden roll up occurs.

Received Sept. 27, 1993; accepted for publication June 3, 1994. Copyright © 1994 by the American Institute of Aeronautics and Astronautics, Inc. All rights reserved.

*Lecturer, Department of Engineering.
†Research Student, Department of Engineering.

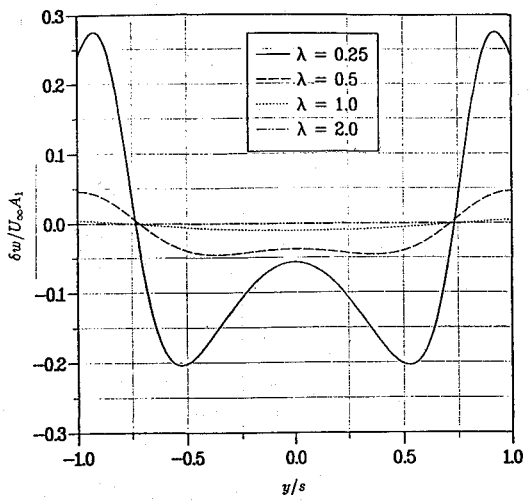

Fig. 1 Induced downwash over the wing due to crossflow vortices.

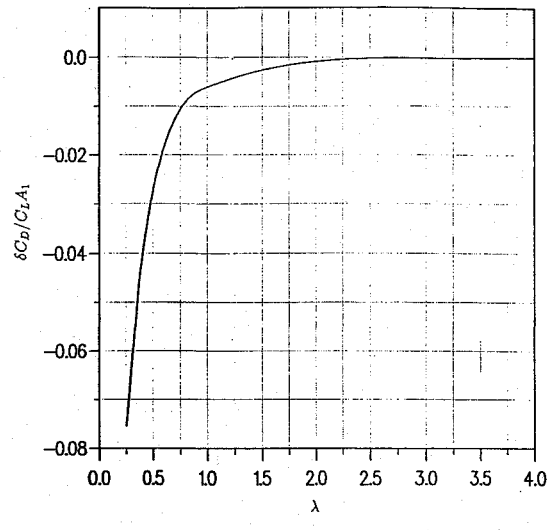

Fig. 2 Induced drag increment due to crossflow vortices.

A roll-up model using continuous vortex lines is considered here. At the roll-up position the vortices from the trailing vortex sheet are assumed to turn across the flow and merge into the two discrete trailing vortices. There are then three contributions to the induced downwash on the wing. The two contributions from the vortex sheet and the discrete trailing vortices are analyzed by Lam[1] and the remaining contribution, analyzed here, is that due to the trailing vortices in the crossflow direction. Inboard of the two discrete trailing vortices the crossflow vortices are in the same direction as the wing bound vortex whereas outboard the opposite applies. The inboard crossflow vortices, therefore, produce upwash over the wing whereas the outboard vortices produce downwash. From the Biot–Savart law the induced downwash velocity increment δw at a spanwise position y' on the wing is given by

$$\delta w = -\frac{1}{4\pi}\int_{-s}^{s} \frac{G\ell}{[(y - y')^2 + \ell^2]^{3/2}}\,dy \qquad (1)$$

where $G(y)$ denotes the spanwise circulation distribution of the crossflow vortices. In Eq. (1) s is the wing semispan. In terms of the wing spanwise circulation distribution $\Gamma(y)$, $G(y) = -\Gamma(y)$ outboard of the two discrete trailing vortices and inboard $G(y) = \Gamma_{y=0} - \Gamma(y)$.

The downwash distributions have been calculated at the values of $\lambda(= \ell/s)$ used by Lam[1] and are shown in Fig. 1 where the down-

wash velocity has been normalized by $U_\infty A_1$ which is the constant value obtained from classical lifting-line theory with elliptic loading. As expected upwash is produced inboard, and downwash is produced outboard with the overall effect being a reduction in drag. This is shown in Fig. 2 where the induced drag increment has been normalized by the value obtained from classical lifting-line theory with elliptic loading. The reduction in drag augments the values determined by Lam[1] and is particularly significant at low values of the roll-up distance less than about one wing span.

Reference

[1]Lam, F., "Induced Drag of Wings of Finite Aspect Ratio," *AIAA Journal*, Vol. 31, No. 1, 1993, pp. 396–398.